LIMNOLOGY and OCEANOGRAPHY

ASLO

Limnol. Oceanogr. 68, 2023, 1147–1160

doi: 10.1002/lno.12335

The global contribution of seasonally migrating copepods to the biological carbon pump

Jérôme Pinti,[1*] **Sigrún H. Jónasdóttir**,[2] **Nicholas R. Record**,[3] **André W. Visser**[2,4]

[1]College of Earth, Ocean, and Environment, University of Delaware, Lewes, Delaware
[2]Section for Ocean and Arctic, Technical University of Denmark, Kongens Lyngby, Denmark
[3]Bigelow Laboratory for Ocean Sciences, East Boothbay, Maine
[4]VKR Centre for Ocean Life, Technical University of Denmark, Kongens Lyngby, Denmark

Abstract

Every year, large numbers of zooplankton migrate from the surface ocean to depths of 500–2000 m to hibernate. Through this migration, they actively transport organic carbon to the deep ocean, where it is used to fuel metabolic needs. This active transport of carbon is thought to be highly efficient, as carbon metabolized by copepods is directly injected deep into the ocean's interior. The significance of this process in view of global carbon cycling remains an open question. Here, we focus on five representative, diapausing copepod species (*Calanus finmarchicus*, *Calanus hyperboreus*, *Calanoides acutus*, *Calanoides natalis*, and *Neocalanus tonsus*) distributed in the Arctic, Atlantic, Indian, and Southern Oceans. For each species, we compute both carbon injection (how much carbon is transported below the euphotic zone during zooplankton migration and left there as dissolved inorganic carbon) and carbon sequestration (the amount of carbon stored in the ocean's interior following diapausing zooplankton-mediated injection). In total, the five species considered here contribute 0.4–0.8% of total biological carbon export, and 0.8–3.3% of total carbon sequestration mediated by the biological pump (assuming a total carbon export of $\sim$ 10 PgC yr^{-1} and sequestration of $\sim$ 1300 PgC). Including other species in this inventory would increase the contribution of diapausing copepods to the biological carbon pump, but requires more precise estimates of copepods' distribution, abundance, and metabolic requirements.

A conspicuous feature of pelagic ecosystems are the annual vertical migrations of large populations of copepods from the oceans' surface to depths of 1000 m or more where they enter diapause for several months of the year (Kaartvedt 1996; Visser and Jónasdóttir 1999; Record et al. 2018). Although most prevalent in high latitude seas, this migration strategy is also found in other parts of the world's oceans and is understood to be an adaptation to extreme seasonal variations in environmental conditions (Williams-Howze 1997) likely dependent on temperature and food availability (Johnson et al. 2008). It is noteworthy that in many of the ecosystems where these seasonal vertical migrants are found, they play a key role in the annual cycles of productivity, acting as a trophic vector between primary producers and higher trophic levels. Furthermore, the sheer numbers involved suggest that these migrants also contribute significantly to the biological carbon pump and the marine carbon cycle (Bradford-Grieve et al. 2001; Kobari et al. 2003; Jónasdóttir et al. 2015; Visser et al. 2017). Specifically, copepods migrating to depths are filled with lipid-rich wax esters that they slowly consume during diapause, injecting respired carbon directly into the deep ocean. Furthermore, copepods suffer from mortality at depths, via predation, starvation, or pathogens (Visser et al. 2017), or because their life cycle imposes that they expire at depths after reproduction (Bradford-Grieve et al. 2001), adding even more carbon injection at depths.

There have been several studies estimating the amount of carbon injected to depth by seasonal vertical migrants. Longhurst and Williams (1992) estimated that carbon export mediated by diapausing copepods was around 0.3 gC m^{-2} yr^{-1} in the North Atlantic, but more recent studies revised this estimate. In the North Atlantic, *Calanus finmarchicus* is now

*Correspondence: pintijerome@gmail.com

Additional Supporting Information may be found in the online version of this article.

Author Contribution Statement: J.P., S.H.J., and A.W.V. prepared abundance and distribution data. J.P. computed carbon export and sequestration. J.P., S.H.J., N.R.R., and A.W.V. analyzed the results. J.P. wrote the manuscript with contributions from all authors.

estimated to export between 1 and 4 gC m^{-2} yr^{-1} (Jónasdóttir et al. 2015), and *Calanus hyperboreus* to export between 3.5 and 6 gC m^{-2} yr^{-1} (Visser et al. 2017). In subantarctic waters and immediately north of the subtropical front, *Neocalanus tonsus* is estimated to export 1.7–9.3 gC m^{-2} yr^{-1}. On a global scale, a recent modeling study (Record et al. 2018) estimated that diapausing copepods were exporting at a minimum between 0.03 and 0.25 PgC yr^{-1}. Their lower bound doubled previous estimates (Longhurst and Williams 1992), with the upper bound substantially higher. Nevertheless, the export appears to be limited compared to the total export mediated by the biological carbon pump (i.e., in addition to seasonal vertical migrations, includes diel vertical migrations and passive sinking of detritus such as fecal pellets and dead organisms). Current global export estimates at the base of the euphotic zone range between 4 and 12 PgC yr^{-1} (Henson et al. 2011; Siegel et al. 2014), with several estimates clustered around 9–10 PgC yr^{-1} (Schlitzer 2002; Dunne et al. 2005; DeVries and Weber 2017).

Export flux, however, is not the only measure of the biological pump. An arguably more important metric is carbon sequestration, that is, the amount of carbon (e.g., PgC) stored in the oceans' interior at equilibrium because of a specific process (Boyd et al. 2019). This depends on where, and at what depth, the carbon is released in the water column. As such, seasonal vertical migrants, that inject carbon directly at depths and often in areas of deep-water formation, may mediate the sequestration of much more carbon than their export flux might suggest. Specifically, recent estimates suggest that 1300 PgC are sequestered in the global ocean via the respiration of organic matter (Carter et al. 2021), that is, sinking aggregates, fecal pellets, and respiring vertical migrants. It is against this background that we seek to estimate how much carbon is sequestered by seasonally migrating copepods.

Here, we provide estimates of carbon export and sequestration for representative copepod populations spanning the globe. Using published copepod abundance data (Smith 1982; Atkinson 1991; Bradford-Grieve et al. 2001; Heath et al. 2004; Verheye et al. 2005; Kvile et al. 2018), and coupling them to a trait-based model of metabolic expenditure at depths (Visser et al. 2017), we compute the total carbon export for *C. finmarchicus* and *C. hyperboreus* in the North Atlantic and the Arctic Ocean, for *N. tonsus* and *Calanoides acutus* in the Southern Ocean, and for *Calanoides natalis* (previously called *C. carinatus*) in the Arabian Sea and the Angola Current. We then couple our results with an ocean circulation inverse model (OCIM) (DeVries and Weber 2017; DeVries and Holzer 2019; Holzer et al. 2021), to compute the total carbon sequestration mediated by the seasonal vertical migrations of these different populations.

Methods

Copepod abundance, diapause depth, and life cycle

The literature was searched for copepod species that are known to enter diapause, and where sufficient information was available (abundance, depth and duration of diapause, and geographical distribution) for model parameterization. The final data compilation are often a combination of several studies (which are referenced in the subsections below). All abundances used here are based on net sampling. Only information that gave vertically resolved abundances during the time of diapause were used, when over 50% of the population were below the mixed layer depth. Development stages were noted, and information on size at stages, abundance, and diapause depth compiled. Areas of distribution used are based on listed appearance of the species.

Two main diapause categories are considered in this study: overwintering of polar/subpolar copepods and monsoon/upwelling driven diapause of tropical/subtropical copepods. The polar copepods have 1-yr to multiyear life cycles, while the tropical species have multiple life cycles per year at the surface during the upwelling season and enter diapause during the termination of the upwelling, usually as stage C5. Here, we are only interested in individuals that do enter diapause during their life. All species that enter diapause store lipids in the form of wax esters in an internal sac and can remain in diapause for over 6 months (Saumweber and Durbin 2006; Baumgartner and Tarrant 2017).

We found sufficient information (especially regarding distribution and abundance) for use in our study for five species from three genera: *Calanoides*, *Calanus*, and *Neocalanus*. Other species (e.g., *Calanus glacialis* in the Arctic Ocean, *Neocalanus flemingeri*, *Neocalanus plumchrus*, and *Neocalanus cristatus* in the North Pacific Ocean) are likely to be of interest, but their distribution and abundance records were too patchy to include them in this study (Fulton 1973; Miller et al. 1984; Miller and Clemons 1988; Miller and Terazaki 1989; Tsuda et al. 2001; Feng et al. 2018).

Calanus finmarchicus

C. finmarchicus typically has a 1-yr life cycle (Fig. 1a). In some cases, *C. finmarchicus* can have multiple generations per productive season, but only the last generation of the summer enters diapause. At the end of summer, C5 copepodites migrate down to 400–1400 m, where they enter diapause before returning to the surface during the following spring (Heath et al. 2000). *C. finmarchicus* was the species for which most abundance data could be found (Heath et al. 2004). Three-dimensional (3D) abundance data were available following sampling of the *C. finmarchicus* distribution area during wintertime, with a vertical resolution of 200 m (Heath et al. 2004). The depth-integrated abundance of diapausing copepods is pictured in Fig. 2a. Heath et al. (2004) constrained their distribution around their sampling locations for higher confidence, but they also extrapolated the 3D *C. finmarchicus* abundance fields over some of its distribution range. Here, we computed export estimates based on both abundance fields: the more conservative one that Heath et al. (2004) and Jónasdóttir et al. (2015) used (within the red polygon of

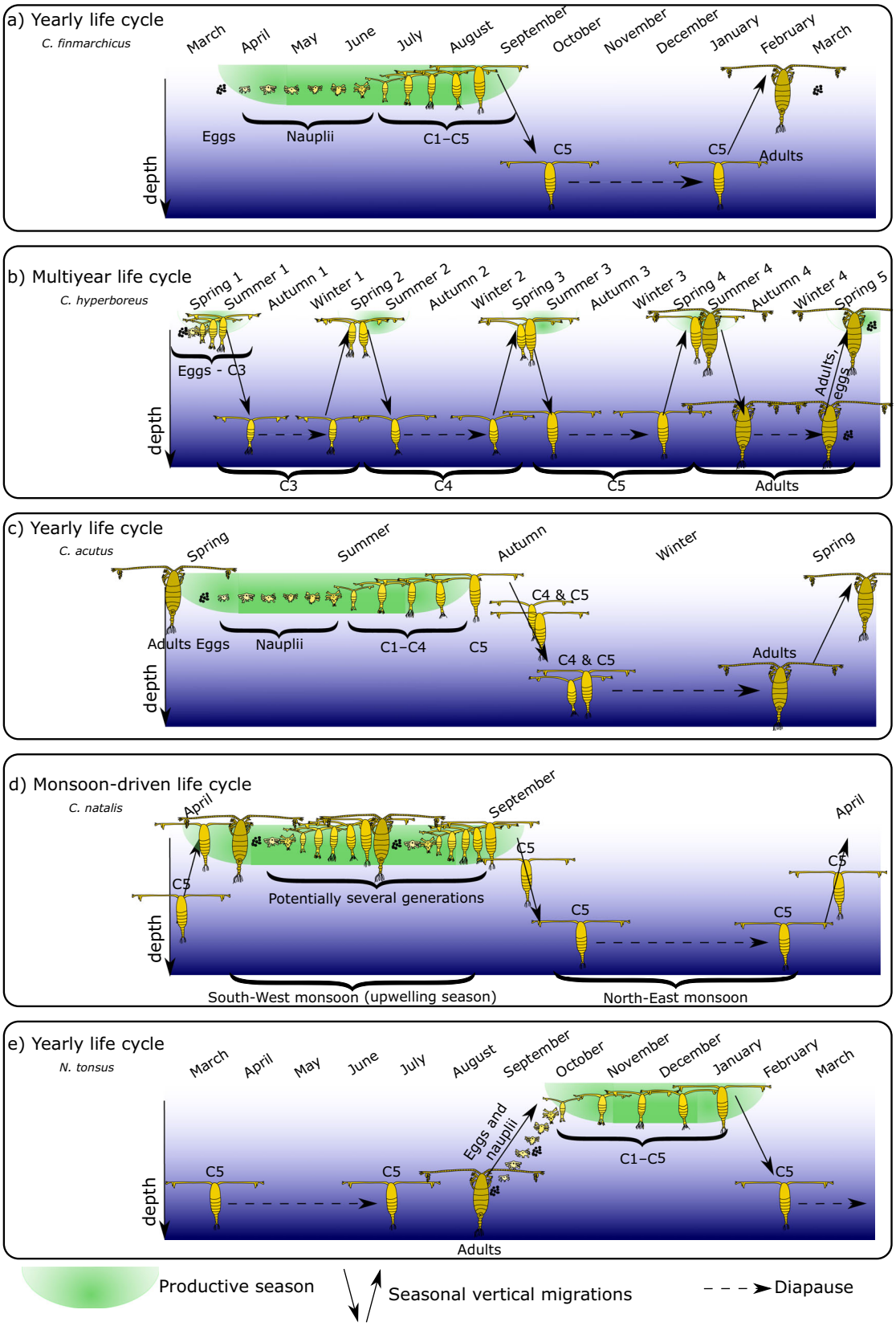

(Figure legend continues on next page.)

Fig. 2a), and the field extended over a larger fraction of the *C. finmarchicus* distribution (also produced by Heath et al. (2004)).

Calanus hyperboreus

C. hyperboreus has a multiyear life cycle (Fig. 1c; Hirche 1997). At the end of summer, C3, C4, C5 copepodites, and adults enter diapause for the winter, where they remain at depths of 600–1500 m (Hirche 1997). Reproduction occurs at depth, and eggs drift toward the surface developing through several life stages on the way. What happens to adults after reproduction is not clear (Visser et al. 2017). The general consensus seems to be that adults expire at depth after spawning, however, observations of spent *C. hyperboreus* females in surface waters in spring suggests that at least some fraction may ascend and go through a second overwintering and reproduction cycle (Swalethorp et al. 2011; Hirche 2013). Following Visser et al. (2017), we assumed that 50% of adults die at depth following reproduction.

Spatial distribution of *C. hyperboreus* (Fig. 2b; *see* Supporting Information Fig. S1 for stage-specific abundances of organisms entering diapause) was obtained for its different stages with a data-constrained two-dimensional (2D) species distribution model (Kvile et al. 2018).

Calanoides acutus

C. acutus is a Southern Ocean species with a 1-yr life cycle (Atkinson 1991). It is one of the few calanoid copepods in the Southern Ocean that truly enters diapause, and it spends up to 9 months at depths (Drits et al. 1994). Nauplii and early copepodite stages reside near the surface, and C4 and C5 copepodites migrate down during late summer/early autumn (Atkinson 1991; Atkinson et al. 1997). Around 30% of copepodites enter diapause as C4 and 70% as C5, and 30% of C5 molting into male adults at depth die after reproduction (Tarling et al. 2004). Females ascend to the surface to spawn at the end of diapause.

C. acutus is distributed in the Antarctic circumpolar current, at least between the Northern extent of the Antarctic Polar Front and the 2000 m isobath (Atkinson 1991; Fig. 2c). To our knowledge, there is no spatially resolved distribution of *C. acutus*; hence, we assumed that they were uniformly distributed within this area, with a conservative estimate of 1000 individuals m^{-2} (Atkinson 1991; Tarling et al. 2004).

Calanoides natalis

C. natalis (previously confused with *C. carinatus*, which is a different species, Bradford-Grieve et al. 2017) is a dominant species in productive coastal upwelling regions on the Western coast of Africa and off Somalia in the Indian Ocean (Smith 1982; Verheye et al. 2005). In the Indian Ocean in particular, its life cycle is tightly linked to the Monsoon cycles and their associated upwellings. When water productivity decreases following nutrient depletion and mixing with the surrounding oligotrophic waters, C5 copepodites descend to depths below 400 m and enter diapause (Verheye et al. 2005). At the onset of a new upwelling event, these C5s terminate diapause and are returned onto the shelf with the upwelled water (Verheye et al. 1992). They molt to the adult stage and reproduce, feeding on the developing phytoplankton bloom. Several generations can be completed at the surface during the upwelling season (Houghton and Mensah 1978).

We focused this study on two upwelling areas with well reported abundances of *C. natalis* (Fig. 2d) along the Somali Coast (mean abundance of diapausing copepods of 30,000 individuals m^{-2}) and off Angola (85,000 individuals m^{-2}) (Verheye et al. 2005).

Neocalanus tonsus

N. tonsus has a 1-yr life cycle (Fig. 1). Nauplii and early copepodite stages develop in the surface layers, and C5 copepodites enter diapause at the end of the austral summer. C5s develop into adults and reproduce at depth. Females spawn lipid-rich, positively buoyant eggs at depth that will float toward the surface and hatch on their way. After reproduction and spawning, adults expire at depth, thus actively contributing to carbon export with the entire adult biomass every year (Bradford-Grieve et al. 2001).

N. tonsus has a circumpolar distribution (Voronina 1975; Bradford-Grieve et al. 2001). However, its distribution is likely patchy and, to our knowledge, no spatially resolved distribution of this species exist. Because of the relatively high abundances of *N. tonsus* reported, we decided to investigate the export of this species where we have the highest data coverage, that is, between 147°E and 156°W (Fig. 2e). Following Bradford-Grieve et al. (2001), we distinguish three areas with different abundances: a 5° band north of the Subtropical Front, a 2° band at the Subtropical Front, and the area between the Subtropical Front and the Antarctic Convergence.

Carbon injection rates

Our aim is to inventory all carbon that is injected at depths once individual copepods enter diapause. The relevant parameters for these calculations are abundance and distribution, respiration rate, diapause depth and duration, mortality rate, and reproductive strategy. Other aspects of the population dynamics (e.g., life cycle and timing of seasonal vertical migration), while of interest, are not of immediate relevance for carbon sequestration and are thus not resolved.

(Figure legend continued from previous page.)

Fig. 1. Representative life cycles of the copepod species considered here. (**a**) *Calanus finmarchicus* depicted here for a 1-yr life cycle and is typical for the North Atlantic, (**b**) *Calanus hyperboreus* in the Arctic Ocean and subpolar North Atlantic, (**c**) *Calanoides acutus* in the Southern Ocean, (**d**) *Calanoides natalis* off the Somali Coast, and (**e**) *Neocalanus tonsus* in the Southern Ocean.

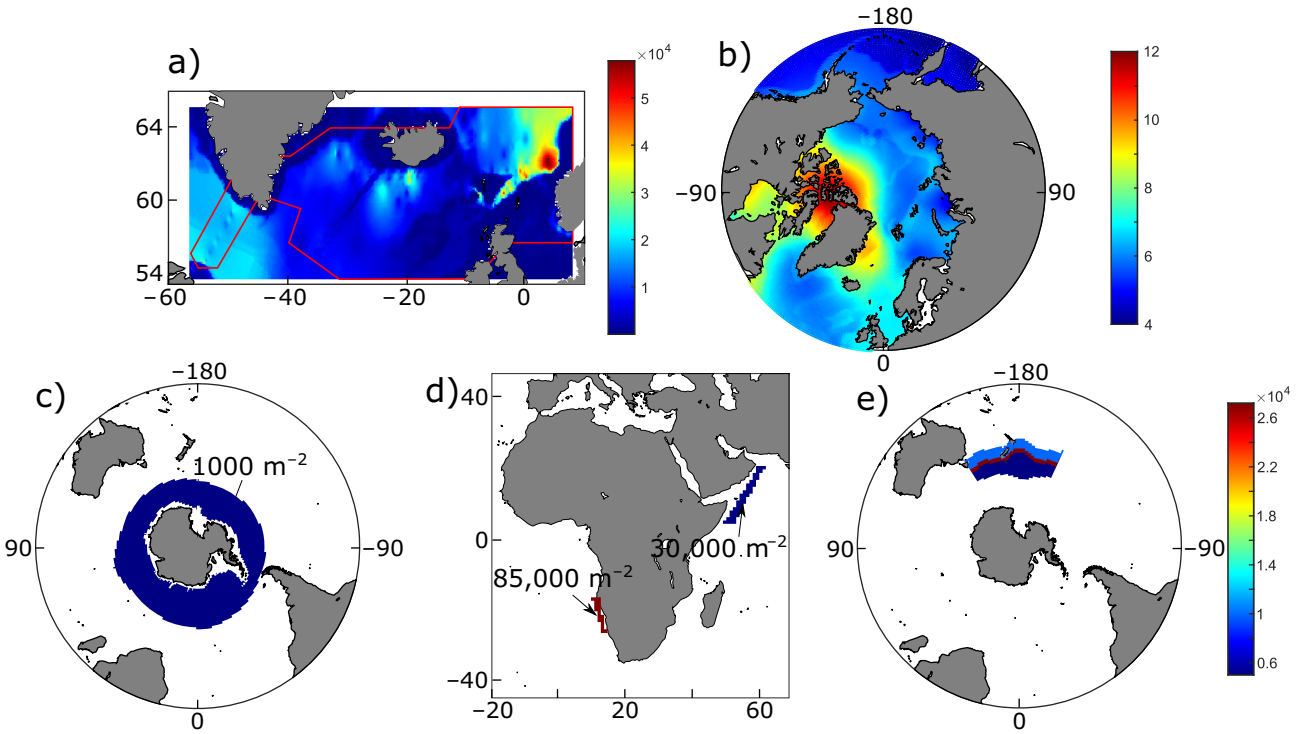

Fig. 2. Abundance of (**a**) *Calanus finmarchicus*, (**b**) *Calanus hyperboreus*, (**c**) *Calanoides acutus*, (**d**) *Calanoides natalis*, (**e**) *Neocalanus tonsus*. For (**a**), the red line shows the core study area of Heath et al. (2004), the rest being areas were abundances were extrapolated. Units are diapausing individuals m^{-2}, expect for *C. hyperboreus*, where unit is $\ln(\text{diapausing individuals } m^{-2})$. Colorbars were specified only for species with locally resolved abundances. Median estimates are specified for the other species.

Diapausing copepods inject carbon at depth via several mechanisms (Fig. 3). First, organisms release dissolved inorganic carbon (DIC) as they respire (Bradford-Grieve et al. 2001; Jónasdóttir et al. 2015; Visser et al. 2017). Second, organisms can die during diapause, and carbon from both their structural body and their lipid sac sinks and gets remineralized to DIC by bacteria. Mortality can be accidental (because of starvation or pathogens; Daase et al. 2014) or obligated: in some species adults die at the end of their diapause (Bradford-Grieve et al. 2001; Visser et al. 2017).

Carbon injection refers to the production of DIC by either of these pathways (Boyd et al. 2019). In this case, because carbon is injected deep into the water column, carbon injection is equal to carbon export (i.e., the amount of carbon that is transported below the euphotic depth). Note that this is not always the case as sinking material can be brought back to the surface by, for example, vertically migrating detritivores.

To compute the carbon injection mediated by diapausing copepods, we use a mechanistic model relying on individual mass (and max. lipid mass) and in situ temperature (Visser et al. 2017). The 3D temperature field used is a climatology produced by the World Ocean Atlas 2018 (Locarnini et al. 2019).

Following Visser et al. (2017), we assume that metabolic rates scale only with structural mass m, and the lipid mass w is used, in part, to cover metabolic expenses. The respiration rate r of a diapausing copepod is:

$$r(m,T) = bm^{3/4}\exp\left(\frac{E(T-T_0)}{kTT_0}\right) \quad (1)$$

with T the temperature, b the metabolic rate coefficient for dormancy, E the activation energy, T_0 the base temperature (in K) and k the Boltzmann constant. All parameters (and their values and units) are summarized in Table 1.

We assume that the emergence from diapause is initiated when (1) the reserve reaches a critical fraction δ of the total body mass (Saumweber and Durbin 2006; Maps et al. 2010; Visser et al. 2017), or when (2) a diapause duration $d_{\max}$ is reached. As such, δ acts as a backstop to diapause when an individual's reserves are reaching this critical threshold. Maximum diapause durations $d_{\max}$ are species-specific and are summarized Table 2.

Assuming a linear decrease in lipid reserves over time with a slope equal to $r(m,T)$ (Visser et al. 2017), diapause length d is equal to:

$$d = \min\left(\frac{(1-\delta)w}{r(m,T)}, d_{\max}\right) \quad (2)$$

Overall, with a concentration c of copepods, the population-integrated respiration over a diapause cycle is:

$$R = crd \tag{3}$$

Assuming that mortality due to starvation and pathogens is evenly distributed throughout diapause, expiring organisms respire, on average, half the carbon that they would need during the diapause, leading to a population-integrated mortality M (Visser et al. 2017):

$$M = \mu cd(m + w - rd/2) \tag{4}$$

with μ the mortality rate during diapause.

The fraction ξ of females that die at depth after diapause (or males that die after reproduction in the case of *C. acutus*) leads to an increased export F (Visser et al. 2017):

$$F = \xi c_f d \frac{\mu \exp(-\mu d)}{1 - \exp(-\mu d)} \max(m + w - rd - C_{egg}, 0) \tag{5}$$

with c_f the concentration of adult females (males for *C. acutus*), and C_{egg} the amount of carbon that a female allocates to egg production at depth (0 for *C. acutus* and females of species that spawn near the surface).

All considered, the total carbon injection mediated by a diapausing population in the water column is:

$$I = \int_z (R + M + F)\, dz \tag{6}$$

Carbon sequestration

Carbon injection was computed as the flux of DIC released at depth by diapausing copepods. Carbon sequestration is the amount of DIC that is stored in the ocean's interior following injection (considered at steady state here). Sequestration estimates are more representative than flux estimates, as a high export flux does not necessarily correlate with a high sequestration flux (Pinti et al. 2022).

Carbon sequestration is computed by estimating the amount of DIC that is stored in the ocean's interior, taking into account the location of DIC release and the ocean's circulation (DeVries et al. 2012). In our case, copepod respiration directly releases DIC, but copepod mortality (both during diapause and after spawning for females) releases particulate organic carbon. As this organic carbon sinks, it gets degraded into DIC by bacterial respiration.

The first step to estimate the depth-dependent injection of DIC by bacterial degradation of particulate organic carbon is to compute the equilibrium distribution of detritus in the water column. This was done by finding the equilibrium of the following transport equation:

$$\frac{\partial D}{\partial t} = -\gamma(z)D - u\frac{\partial D}{\partial z} + S = 0 \tag{7}$$

with D the concentration of sinking detritus (in our case, the decaying carcasses of copepods), γ the bacterial degradation rate of detritus, u the detritus sinking speed, and S the source term of detritus (i.e., M or F). This equation is solved numerically by an Euler scheme. Then, the depth-dependent DIC production is simply $D(z)\gamma(z)$. γ is defined as:

$$\gamma(z) = 0.25 Q_{10}^{\frac{T - T_{ref}}{10}} \tag{8}$$

with Q_{10} the temperature coefficient and T_{ref}(°C) the reference temperature (Bopp et al. 2013; Laufkotter et al. 2015; DeVries and Weber 2017; Pinti et al. 2022; Serra-Pompei et al. 2022).

Carbon sequestration was estimated by coupling the DIC source terms with an ocean circulation model. We used OCIM (Holzer et al. 2021). We selected OCIM for two main reasons. First, OCIM is a transport matrix model, which is computationally efficient compared to heavy ocean general circulation

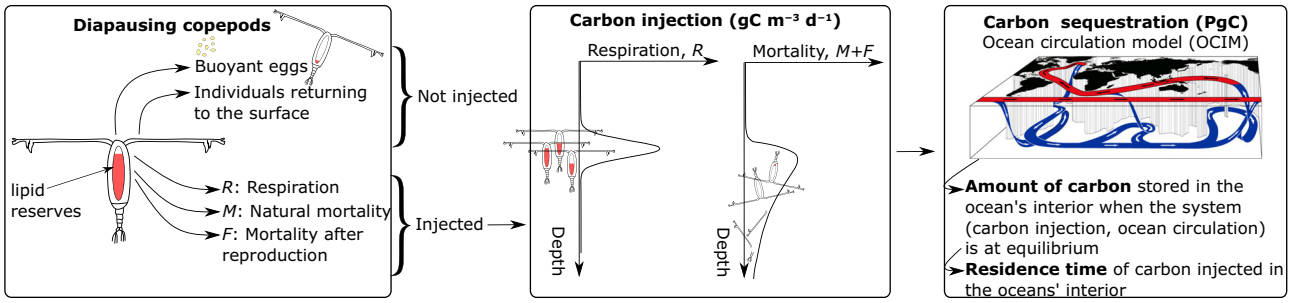

Fig. 3. Outline of the model. A diapausing copepod will use its carbon mass (both structural and lipids) to respire or create buoyant eggs. It can also die or terminate diapause and migrate back to surface waters. Only carbon that remains at depth is ultimately transformed into DIC (either directly via copepod respiration or through bacterial degradation of carcasses) and thus injected in the oceans' interior. By coupling OCIM, and ocean circulation model, to our carbon injection, we estimate how much carbon is sequestered via seasonal vertical migrations as well as its residence time scale. Illustration in the 3rd panel is adapted from Neelin (2011).

Table 1. Glossary of parameters and variables.

Parameter	Value	Unit	Signification
A	—	d^{-1}	Advection–diffusion matrix transport operator from OCIM
b	$2.5–5 \times 10^{-7}$*	$\mu gC^{0.25}\ s^{-1}$	Metabolic rate coefficient for dormancy
c	—	ind m^{-3}	Copepod abundance
c_f	—	ind m^{-3}	Adult female abundance
C_{egg}	Table 2	μgC	Total carbon in spawned eggs
C_{in}	Eq. 9	gC m^{-3}	DIC concentration
d	Eq. 2	d	Diapause duration
D	Eq. 7	gC m^{-3}	Detritus concentration in the water column
d_{max}	Table 2	d	Maximum diapause duration
E	0.6	eV	Activation energy for copepod diapause respiration
F	Eq. 5	gC $m^{-3}\ yr^{-1}$	Mortality of females after spawning
I	Eq. 6	gC $m^{-2}\ yr^{-1}$	Total carbon injection
J_{res}	γD	gC $m^{-3}\ d^{-1}$	Source term of DIC
k	8.61733×10^{-5}	eV K^{-1}	Boltzmann constant
m	Table 2	μgC	Structural mass of a copepod
M	Eq. 4	gC m^{-3} yr	Mortality during diapause
p	Table 2	mm	Prosome length
Q_{10}	2	—	Temperature coefficient for microbial degradation of detritus
r	Eq. 1	$\mu gC\ s^{-1}\ ind^{-1}$	Respiration rate
R	Eq. 3	gC $m^{-3}\ yr^{-1}$	Respiration during diapause
S	M or F	gC $m^{-3}\ d^{-1}$	Source term of detritus
T	—	K	Temperature
T_0	273	K	Base temperature
T_{ref}	5	°C	Reference temperature for bacterial degradation
u	Table 2	m d^{-1}	Sinking speed of carcasses
w	Table 2	μgC	Maximum wax ester mass for a copepod
z	—	m	Depth
γ	Eq. 8	d^{-1}	Bacterial degradation rate
δ	0.2	—	Minimum wax ester fraction
μ	0.001	d^{-1}	Natural mortality rate
ξ	Table 2	—	Fraction of females that die at depth after spawning

*Values for all copepods, except for *Calanoides natalis* for which b was varied between 2 and $3 \times 10^{-8}\ \mu gC^{0.25}\ s^{-1}$ to ensure consistency with Verheye et al. (2005).

models, and enables for quick computation of equilibrium solutions (Khatiwala et al. 2005). Second, OCIM was specifically constrained with radiocarbon ($\Delta^{14}C$) and helium isotopes (δ^3He) tracers for a better representation of deep-sea circulation and ventilation rates (DeVries and Holzer 2019), a crucial feature of the model considering the depth at which diapausing copepods reside. Fitting circulation model to observed tracers is a way to reduce model errors due to circulation biases and to guarantee a good representation of water mass structure and interior ocean ventilation rates (Doney et al. 2004; DeVries and Weber 2017).

We computed the equilibrium concentration of DIC C_{in} with the following equation:

$$\frac{dC_{in}}{dt} = \mathbf{A}C_{in} + J_{res} = 0 \quad (9)$$

with **A** the advection–diffusion matrix transport operator from OCIM, and J_{res} the DIC source term. This equation was solved assuming instantaneous air–sea CO_2 equilibriation, that is, with a boundary condition $C_{in} = 0$ at the surface. After solving for C_{in}, we volume-integrate over the whole ocean to obtain the total sequestered carbon mediated by the mechanism in focus.

Dividing total carbon sequestration by carbon export yields a sequestration time (in years), a measure of the efficiency of this process of the biological carbon pump. Figure 4 illustrates

Table 2. Glossary of species- and stage-specific parameters. Prosome length is not used in computations and it is provided as an indication of the size of the different organisms considered. For structural mass, lipid mass, sinking speed, and diapause depth parameters, low and high estimates are provided. Estimates of carcasses sinking speed in parenthesis refer to adult females with eggs. Mass of spawned eggs is the total mass of eggs laid by a female during a reproductive event. Parameters are taken from the following studies: *Calanus finmarchicus*: Jónasdóttir et al. (2015), Jónasdóttir et al. (2019); *Calanus hyperboreus*: Visser et al. (2017); *Calanoides acutus*: Atkinson (1991), Kattner et al. (1994), Zmijewska et al. (1999), Pond et al. (2012); *Calanoides natalis*: Smith (1982), Verheye et al. (1992), Verheye et al. (2005); *Neocalanus tonsus*: Ohman et al. (1989), Bradford-Grieve et al. (2001).

Organism	Prosome length (mm)	Structural mass (μgC)	Max lipid mass (μgC)	Max. diapause length (d)	Carcasse sinking speed (m d^{-1})	Mean diapause depth (m)	Std dev. of diapause depth (m)	Frac. dying after reproduction (—)	Mass of spawned eggs (μgC)
C. finmarchicus C5	2.7	39–74	67–127	330	100–200	—	—	—	—
C. hyperboreus C3	2.5	63–63	108–108	240	50–100	600–1500	50–100	—	—
C. hyperboreus C4	4.0	165–269	283–461	240	100–200	600–1500	50–100	—	—
C. hyperboreus C5	6.0	383–907	656–1555	240	200–500	600–1500	50–100	—	—
C. hyperboreus C6f	7.0	1001–1441	1716–1977	240	250–800 (300–1000)	600–1500	50–100	0.5	900
C. hyperboreus C6m	6.5	907–1153	1555–2470	240	200–600	600–1500	50–100	0.5	—
C. acutus C4	2.4	45–57	121–202	195	50–100	500–800	50–100	—	—
C. acutus C5	3.7	50–151	240–400	195	100–200	500–800	50–100	0.3 (males only)	—
C. natalis C5	2.0	30–40	42–54	195	50–100	500–750	50–100	0	—
N. tonsus C5	2.4	70–130	220–280	195	50–100	750–1000	50–100	-	—
N. tonsus C6	4.1	100–200	100–160	45	80–200 (100–500)	750–1000	50–100	1	92

how sequestration time varies across the world, assuming that carbon is respired around 1000 m. This sequestration time is only dependent on ocean circulation (captured by OCIM), and not on the actual amount of carbon respired at depth as carbon sequestered is then divided by export. Sequestration time is much higher in areas of deep-water formation, such as around Antarctica or in the Arctic. Notably, these areas are also important grounds for diapausing copepods, suggesting that diapausing copepods might be efficient at sequestering carbon on a long time scale.

Results

Many of the parameters used in this model are poorly constrained (copepod abundances, metabolic rates, diapause depth, structural, and lipid mass at the onset of diapause). As such, we do not aim to provide definitive estimates of carbon injected, sequestration, and sequestration time by diapausing copepods. Rather, we provide upper and lower bounds of estimates of injection, sequestration, and residence time for the different copepod populations considered. We ran the model for all possible combinations of parameter estimates, and the results provided correspond to the lower and higher estimate obtained within these simulation arrays.

Copepod species considered here each inject a relatively modest amount (between 0.3 and 28×10^{12}gC yr^{-1}) in the ocean's interior during diapause (Fig. 5; Table 3). The species with the lowest export per area is *C. acutus*, exporting between 0.13 and 0.46 gC m^{-2} yr^{-1}, while *N. tonsus* exports between 2.54 and 3.68 gC m^{-2} yr^{-1}—the highest export among the species investigated here. These export values are consistent with computed values for diapausing copepods: between 1.6 and 6.4 gC m^{-2} yr^{-1} for *C. finmarchicus* (Jónasdóttir et al. 2015), between 0.3 and 3.6 gC m^{-2} yr^{-1} for *C. hyperboreus* (Visser et al. 2017), and between 1.7 and 9.3 gC m^{-2} yr^{-1} for *N. tonsus* (Bradford-Grieve et al. 2001).

On a global scale, the total export of the five species considered here (including the extended *C. finmarchicus* area) ranges between 0.036 and 0.075 PgC yr^{-1}. Although we do not have an exhaustive assessment of carbon export mediated by all diapausing copepods as we only focus on five different species, this estimate is in line with a previous global estimate of the lower bound of carbon export mediated by diapausing copepods—evaluated to range between 0.03 and 0.25 PgC yr^{-1} (Record et al. 2018).

The sequestration potential of the five different species vary by approximately one order of magnitude, consistently with total export. *C. natalis* sequesters between 0.1 and 0.7 PgC, while *C. hyperboreus* sequesters between 7.5 and 15.5 PgC (Table 3). However, when normalized per distribution area, carbon sequestered is more similar across copepod species: *C. natalis* sequesters 160–960 gC m^{-2}, and *C. hyperboreus* 470–970 gC m^{-2}. This leads to similar sequestration time scales, ranging from 157–311 yr for *N. tonsus* to 430–750 yr for *C.*

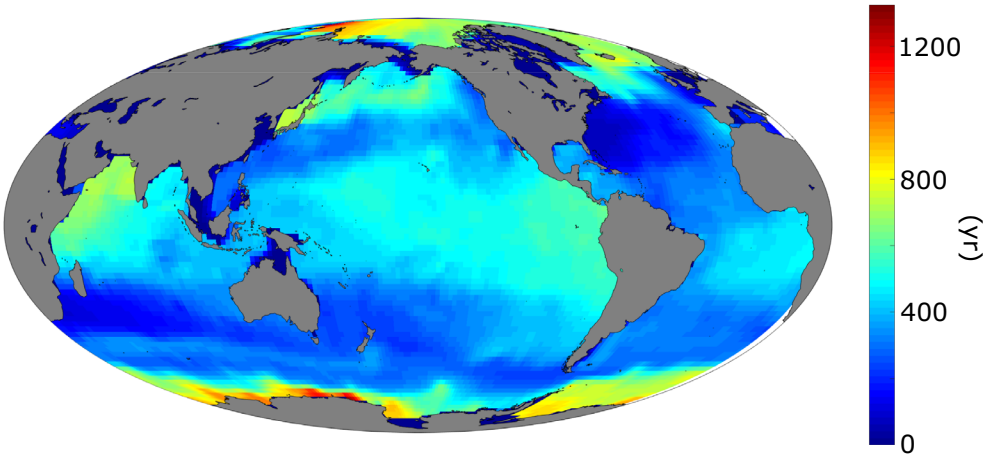

Fig. 4. Sequestration time (years) of carbon injected at 1000 m depth around the globe.

hyperboreus (Table 3). Although the Southern Ocean has a relatively high sequestration time scale for carbon injected at 1000 m (Fig. 4), carbon sequestered via both Southern species (*N. tonsus* and *C. acutus*) has a much lower sequestration time—up to 311 and 510 yr, respectively (Table 3). It is because of their diapause depth (*C. acutus* resides at shallower depths than the 1000 m baseline of Fig. 4) and spatial distribution (here, *N. tonsus* is constrained around New Zealand, where the sequestration time is not as high as in other places of the Southern Ocean).

Carbon sequestered by diapausing copepods does not remain where it was respired. It is transported as DIC by the ocean's global circulation (Supporting Information Fig. S2). *C. finmarchicus* and *C. acutus* (and, to a lesser extent, *C. hyperboreus* and *N. tonsus*) are distributed in areas of deep-water formation, so the resulting carbon is sequestered all around the globe (Supporting Information Fig. S2a–c,e). Conversely, *C. natalis* distribution is not in areas of strong deep-water formation, and the resulting carbon distribution remains more localized (Supporting Information Fig. S2d).

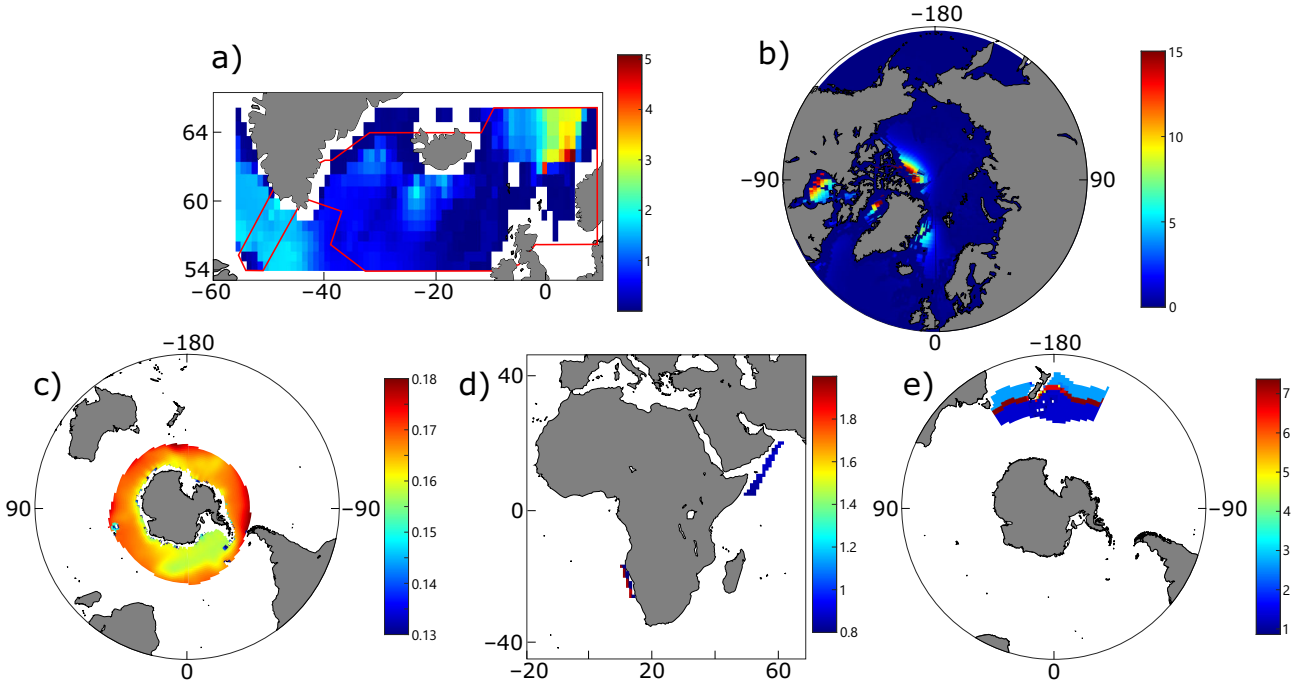

Fig. 5. Export of (**a**) *Calanus finmarchicus*, (**b**) *Calanus hyperboreus*, (**c**) *Calanoides acutus*, (**d**) *Calanoides natalis*, (**e**) *Neocalanus tonsus* in gC m yr^{-1}. Note the different colorbars for the different panels.

Table 3. Summary of results. Note that normalized export and sequestration numbers may not correspond exactly to the numbers in Fig. 5 and Supporting Information Fig. S2 as normalized values are averaged over the entire distribution area. *Calanus finmarchicus* (ext.) refers to the extended distribution pictured in Fig. 2a.

Species	Area (10^6 km^2)	Abundance (#/m^2)*	Mean Biomass (GgC)	Mean biomass (gC m^{-2})	Injection (GgC yr^{-1})	Injection (gC m^{-2} yr^{-1})	Sequestration (PgC)	Sequestration (gC m^{-2})	Sequestration time scale (yr)	Sequestration biomass ratio (–)
C. hyperboreus	16	500–11,500	38–59	2.38–3.71	12–28	0.75–1.75	7.5–15.5	469–969	427–749	197–263
C. finmarchicus	2.9	15,000–40,000	3.4–8.5	1.17–2.93	1.6–5.1	0.55–1.76	0.9–2.7	293–921	514–525	265–318
C. finmarchicus (ext.)	3.8	15,000–40,000	4.9–12	1.29–3.16	2.5–7.8	0.66–2.05	1.2–4.0	318–1039	494–509	245–333
N. tonsus	6.57	5000–27,000	19–26	2.82–3.99	17–24	2.54–3.68	2.7–7.5	405–1145	157–311	142–288
C. acutus	30.7	800–1300	6–19	0.20–0.63	4–14	0.13–0.46	1.5–6.8	50–222	346–510	250–358
C. natalis	0.69	15,000–127,500	1.1–4.4	1.59–6.38	0.3–1.4	0.41–2.03	0.1–0.7	159–957	351–539	91–159

*Abundance ranges are the minimum and maximum of local estimates for *Calanus hyperboreus*, *Calanus finmarchicus*, and *Neocalanus tonsus*, but represent the range of values tested as total abundances for the others (for *Calanoides natalis*, the minimum value corresponds to the minimum abundance in Arabian Sea and the maximum to the maximum abundance off Angola).

Discussion

The five diapausing copepod species considered in this study export between 0.036 and 0.075 PgC yr^{-1} in the ocean's interior, representing only about 0.4–0.8% of the total export mediated by the biological carbon pump (assuming that it ranges around 9–10 PgC yr^{-1}; Schlitzer 2002; Dunne et al. 2005; DeVries and Weber 2017). However, due to their deep residency and strategic location in areas of deep-water formation, the relative importance of diapausing copepods to carbon sequestration is more important. A recent study assessed that the ocean's interior stores 1300 PgC (with a standard deviation of 230 PgC) through organic carbon remineralization (Carter et al. 2021)—suggesting that the five copepod species studied here (sequestering 13–35 PgC) are responsible for 0.8–3.3% of the total carbon sequestered via the biological carbon pump. This shows that the importance of a process to the biological carbon pump is a function not only of its strength (the export), but also of the depth at which the conversion to DIC takes place.

Despite large variations in life cycle (Fig. 1), abundance (from 500 to 40,000 individuals m^{-2}), and study area (from 0.7 to 31 million km^2) for the five species studied here, carbon injection and sequestration time scale in particular appear relatively homogeneous across the five species (Table 3). As larger organisms respire more carbon and have larger carcasses, they naturally contribute more to carbon injection than smaller individuals. However, normalizing carbon injection and sequestration per total biomass give an indication of the efficiency of a species at sequestering carbon. Although this ratio is species specific, it largely hinges on local sequestration time scales (and diapausing depths) rather than on properties of the diapausing animals. All species sequester between 90 and 360 times their carbon weight (Table 3), highlighting their high importance for the biological carbon pump relative to their size. Everything else being equal, it does not seem that the size, life cycle, or reproductive style (*N. tonsus* and *C. hyperboreus* are capital breeders while the other species are largely income breeders) have a major role in either injection or sequestration. One trait that might promote high carbon injection is the obligate expiration at depth of adults after reproduction: of the five species investigated here, *N. tonsus* yields the highest relative export and sequestration of all.

As our study only included five species, and only over part of their range, our results are probably an underestimate of the global importance of diapausing copepods to global carbon sequestration; 13–35 PgC of carbon sequestered may be modest, especially when compared to carbon sequestered by all biological processes (Carter et al. 2021). However, while our analysis included five species with relatively well documented abundances and distributions, many more copepod species undertake seasonal vertical migrations. The Encyclopedia of Life (https://eol.org, accessed 25 August 2022) lists 30 different copepod species undertaking diapause at different

life stages. Considering more species and wider distribution areas would naturally increase the total export and sequestration presented here. For example, *C. glacialis* is another diapausing copepod species in the North Atlantic and the Arctic, and several *Neocalanus* sp. enter diapause in the North Pacific. A local study in the North Pacific (Kobari et al. 2008) estimated that *N. flemingeri* contributed 0.25 gC m^{-2} yr^{-1} to carbon export at 1000 m thanks to their seasonal migration, and that *N. cristatus* and *N. plumchrus* export together more than 1.7 gC m^{-2} yr^{-1}. If these numbers were confirmed on a basin scale, the total contribution of copepods to the biological carbon pump would be significantly higher. Similarly, the distribution of *N. tonsus* was constrained between 147°E and 156°W, as this area is where most records of the species are provided (Bradford-Grieve et al. 2001). However, *N. tonsus* is consistently reported in other areas of the Southern Ocean, suggesting that it has a circumpolar distribution (Voronina 1975; Ohman et al. 1989; Bradford-Grieve et al. 2001). Extending our prescribed distribution of *N. tonsus* across the Southern Ocean leads to an export of 0.12–0.18 PgC yr^{-1}, and a sequestration of 23–62 PgC for this species alone. These very large numbers are likely to be lower in reality, for example, if the abundance of diapausing individuals is lower in other regions of the Southern Ocean than close to New Zealand. Nevertheless, this little exercise suggests that diapausing copepods may contribute significantly more to the biological carbon pump than stated in this study.

Our estimates are highly dependent on sampling coverage (both vertically and horizontally). There are significant gaps in the global understanding of diapausing copepods—particularly in much of the Pacific Ocean, parts of the Arctic and Southern Oceans, and in the South Atlantic. Expanding our knowledge of the distribution of these copepods during diapause would refine our estimates. Out of the five species considered here, we could find a 3D distribution of individuals for only one (*C. finmarchicus*—and only over part of its range), a 2D distribution for another one (*C. hyperboreus*), and we had to take spatially averaged estimates for the others (*N. tonsus* and *C. natalis* areas were divided in three and two different zones, respectively). Other estimates of *C. acutus* exist for specific transects (Ward et al. 2012), and using them would have linearly modified our results as abundance and injection and sequestration are linearly related. Other copepod species that are likely of interest for carbon sequestration such as *Neocalanus* sp. in the North Pacific were not included in this study because of the lack of abundance maps across a significant part of their ranges.

In addition to spatial coverage, results presented here are sensitive to other parameters. Carbon injection (and thus sequestration) is directly proportional to copepod abundances. Everything else being equal, doubling copepod populations would double carbon injection and sequestration (not impacting residence time), making abundance a key parameter for this study. Another important parameter when it comes to copepod carcasses is bacterial degradation rate. Although the degradation rate does not modify carbon injection rates, it modifies the depth at which the carcasse is remineralized, and ultimately the amount of carbon that is sequestered via this pathway. A higher degradation rate means that carbon is injected higher up in the water column, generally leading to a lower carbon sequestration and residence time than with a lower bacterial degradation rate. Similarly, mean diapause depth and copepod respiration rate are important parameters for carbon sequestration via copepod respiration. Diapause depth can be estimated precisely via echosounders or net tows, but copepod respiration rates during diapause can be harder to estimate. For both these parameters (metabolic rate and diapause depth), we used a low and a high estimate for all species (Tables 1, 2) and reported the most extreme values for each run.

Our work only considered that diapausing copepods respire carbon, produce eggs, or die (and thus have their carcasses degraded by bacteria). However, even if mortality risks are greatly reduced compared to surface habitats (Baumgartner and Tarrant 2017), mesopelagic and bathypelagic organisms may still feed on diapausing copepods, linking into Vinogradov's ladder (Vinogradov 1962). Depending on the vertical behavior of these predators, zooplankton predation can alter carbon sequestration (Pinti et al. 2022): if predators stay at the same depth or go deeper, they will inject carbon (either as respired DIC or through fecal pellets that will subsequently be degraded by bacteria) at least as deep as copepods would, thus increasing carbon sequestration. However, if they migrate up during part of the day, carbon will likely be injected in shallower waters (except, maybe, for fast-sinking fecal pellets that will be degraded all along their descent)—thus decreasing carbon sequestration and sequestration time. Carbon export rates are less sensitive to predation: export can increase with predation only if copepods migrate back to the surface after diapause (e.g., *C. finmarchicus* and *C. hyperboreus*), and export can decrease only if predators egest or respire the carbon they ingested at depth in the euphotic zone. This is unlikely to happen for small mesopelagic fish, but could happen for large planktivorous organisms that can forage at depth, such as whale and basking sharks (Doherty et al. 2019; Arrowsmith et al. 2021). The importance of predation for diapausing copepod abundances and their subsequent carbon export and sequestration is currently unknown, but we can posit that it has a limited effect—at least for carbon export.

The biological carbon pump plays an important in climate regulation, as it was estimated that atmospheric pCO_2 would be ~200 ppm higher than the current 400 pm without it (Maier-Reimer et al. 1996). But climate change also disrupts zooplankton abundances, distribution, and phenology (Richardson 2008). Predicting the future of seasonal carbon sequestration is complex, as many effects can arise and cascade through food webs (Pinti et al. 2022), and because of regional variations (Richardson and Schoeman 2004). Higher temperatures increase metabolic rates, thus increasing export per amount of time spent at depth. But higher temperatures

will also trigger earlier blooms, so copepods will have to emerge from diapause earlier at the risk of a mismatch with phytoplankton blooms (Edwards and Richardson 2004)—thus decreasing carbon export. Changes in abundances will directly impact carbon export and sequestration, and changes in zooplankton distribution will alter carbon sequestration. For example, a northward movement of *C. finmarchicus* could push them away from deep-water formation zones in the North Atlantic (thus decreasing sequestration), while a more southern distribution of *N. tonsus* could create an overlap with areas of deep-water formation in the Southern Ocean (similarly to the current distribution of *C. acutus*). Poleward-shifting isotherms could reduce diapause habitat for many species, but the opening of ice-covered oceans could create new diapause habitat. Predicting the future of the biological carbon pump and the lipid shunt will require better estimates of zooplankton abundances, distribution, and metabolic rates so that they could be included in global ecosystem models (Record et al. 2018).

Conclusion

Our study focused on the importance of five diapausing copepods to the biological carbon pumps. Despite limited export flux, diapausing copepods contributed relatively more to carbon sequestration than to carbon export because of their deep residency. High uncertainties remain because of incomplete and scarce abundance records, especially for other species not included in this study—species that are likely to contribute similarly to the biological carbon pump. Finely quantifying the importance of seasonal vertical migrations to the biological carbon pump is an important question for future global ecosystem modeling and climate research.

Data availability statement

The source code (written in MATLAB) supporting this article has been uploaded as part of the Supporting Information and is available at: https://gitlab.com/ud3/seasonal-vertical-migrations-and-carbon-pump/

REFERENCES

Arrowsmith, L., A. Sequeira, C. Pattiaratchi, and M. Meekan. 2021. Water temperature is a key driver of horizontal and vertical movements of an ocean giant, the whale shark *Rhincodon typus*. Mar. Ecol. Prog. Ser. **679**: 101–114.

Atkinson, A. 1991. Life cycles of *Calanoides acutus*, *Calanus simillus* and *Rhincalanus gigas* (Copepoda: Calanoida) within the Scotia Sea. Mar. Biol. **109**: 79–91.

Atkinson, A., S. B. Schnack-Schiel, P. Ward, and V. Marin. 1997. Regional differences in the life cycle of *Calanoides acutus* (Copepoda: Calanoida) within the Atlantic sector of the Southern Ocean. Mar. Ecol. Prog. Ser. **150**: 99–111.

Baumgartner, M. F., and A. M. Tarrant. 2017. The physiology and ecology of diapause in marine copepods. Ann. Rev. Mar. Sci. **9**: 387–411.

Bopp, L., and others. 2013. Multiple stressors of ocean ecosystems in the 21st century: Projections with CMIP5 models. Biogeosciences **10**: 6225–6245.

Boyd, P. W., H. Claustre, M. Levy, D. A. Siegel, and T. Weber. 2019. Multi-faceted particle pumps drive carbon sequestration in the ocean. Nature **568**: 327–335.

Bradford-Grieve, J. M., S. D. Nodder, J. B. Jillett, K. Currie, and K. R. Lassey. 2001. Potential contribution that the copepod *Neocalanus tonsus* makes to downward carbon flux in the Southern Ocean. J. Plankton Res. **23**: 963–975.

Bradford-Grieve, J. M., L. Blanco-Bercial, and I. Prusova. 2017. *Calanoides natalis* Brady, 1914 (Copepoda: Calanoida: Calanidae): Identity and distribution in relation to coastal oceanography of the Eastern Atlantic and Western Indian Oceans. J. Nat. Hist. **51**: 807–836.

Carter, B. R., R. A. Feely, S. K. Lauvset, A. Olsen, T. DeVries, and R. Sonnerup. 2021. Preformed properties for marine organic matter and carbonate mineral cycling quantification. Global Biogeochem. Cycl. **35**: e2020GB006623.

Daase, M., O. Varpe, and S. Falk-Petersen. 2014. Non-consumptive mortality in copepods: Occurrence of *Calanus* spp. carcasses in the Arctic Ocean during winter. J. Plankton Res. **36**: 129–144.

DeVries, T., F. Primeau, and C. Deutsch. 2012. The sequestration efficiency of the biological pump. Geophys. Res. Lett. **39**: 1–5.

DeVries, T., and T. Weber. 2017. The export and fate of organic matter in the ocean: New constraints from combining satellite and oceanographic tracer observations. Global Biogeochem. Cycles **31**: 535–555.

DeVries, T., and M. Holzer. 2019. Radiocarbon and helium isotope constraints on deep ocean ventilation and mantle-3He sources. J. Geophys. Res. Oceans **124**: 3036–3057.

Doherty, P. D., and others. 2019. Seasonal changes in basking shark vertical space use in the north-East Atlantic. Mar. Biol. **166**: 1–12.

Doney, S. C., and others. 2004. Evaluating global ocean carbon models: The importance of realistic physics. Global Biogeochem. Cycles **18**: 1–22.

Drits, A. V., A. F. Pasternak, and K. N. Kosobokova. 1994. Physiological characteristics of the Antarctic copepod *Calanoides acutus* during late summer in the Weddell Sea. Hydrobiologia **292–293**: 201–207.

Dunne, J. P., R. A. Armstrong, A. Gnnadesikan, and J. L. Sarmiento. 2005. Empirical and mechanistic models for the particle export ratio. Global Biogeochem. Cycl. **19**: 1–16.

Edwards, M., and A. J. Richardson. 2004. Impact of climate change on marine pelagic phenology and trophic mismatch. Nature **430**: 881–884.

Feng, Z., R. Ji, C. Ashjian, R. Campbell, and J. Zhang. 2018. Biogeographic responses of the copepod *Calanus glacialis* to a changing Arctic marine environment. Glob. Chang. Biol. **24**: e159–e170.

Fulton, J. 1973. Some aspects of the life history of *Calanus plumchrus* in the strait of Georgia. J. Fish. Res. Board Can. **30**: 811–815.

Heath, M. R., J. G. Fraser, A. Gislason, S. J. Hay, S. H. Jónasdottir, and K. Richardson. 2000. Winter distribution of *Calanus finmarchicus* in the Northeast Atlantic. ICES J. Mar. Sci. **57**: 1628–1635.

Heath, M. R., and others. 2004. Comparative ecology of overwintering *Calanus finmarchicus* in the northern North Atlantic, and implications for life-cycle patterns. ICES J. Mar. Sci. **61**: 698–708.

Henson, S. A., R. Sanders, E. Madsen, P. J. Morris, F. Le Moigne, and G. D. Quartly. 2011. A reduced estimate of the strength of the ocean's biological carbon pump. Geophys. Res. Lett. **38**: 10–14.

Hirche, H. J. 1997. Life cycle of the copepod *Calanus hyperboreus* in the Greenland Sea. Mar. Biol. **128**: 607–618.

Hirche, H. J. 2013. Long-term experiments on lifespan, reproductive activity and timing of reproduction in the Arctic copepod *Calanus hyperboreus*. Mar. Biol. **160**: 2469–2481.

Holzer, M., T. DeVries, and C. de Lavergne. 2021. Diffusion controls the ventilation of a Pacific Shadow Zone above abyssal overturning. Nat. Commun. **12**: 1–13.

Houghton, R., and M. Mensah. 1978. Physical aspects and biological consequences of Ghanaian coastal upwelling, p. 167–180. *In* R. Boje and M. Tomczak [eds.], Upwelling ecosystems. Springer.

Johnson, C. L., A. W. Leising, J. A. Runge, E. J. Head, P. Pepin, S. Plourde, and E. G. Durbin. 2008. Characteristics of *Calanus finmarchicus* dormancy patterns in the Northwest Atlantic. ICES J. Mar. Sci. **65**: 339–350.

Jónasdóttir, S. H., A. W. Visser, K. Richardson, and M. R. Heath. 2015. Seasonal copepod lipid pump promotes carbon sequestration in the deep North Atlantic. Proc. Natl. Acad. Sci. U. S. A. **112**: 12122–12126.

Jónasdóttir, S. H., R. J. Wilson, A. Gislason, and M. R. Heath. 2019. Lipid content in overwintering *Calanus finmarchicus* across the Subpolar Eastern North Atlantic Ocean. Limnol. Oceanogr. **64**: 2029–2043.

Kaartvedt, S. 1996. Habitat preference during overwintering and timing of seasonal vertical migration of *Calanus finmarchicus*. Ophelia **44**: 145–156.

Kattner, G., M. Graeve, and W. Hagen. 1994. Ontogenic and seasonal changes in lipid and fatty acid/alcohol compositions of the dominant Antarctic copepods *Calanus propinquus*, *Calanoides acutus* and *Rhincalanus gigas*. Mar. Biol. **118**: 637–644.

Khatiwala, S., M. Visbeck, and M. A. Cane. 2005. Accelerated simulation of passive tracers in ocean circulation models. Ocean Model. **9**: 51–69.

Kobari, T., A. Shinada, and A. Tsuda. 2003. Functional roles of interzonal migrating mesozooplankton in the western subarctic Pacific. Prog. Oceanogr. **57**: 279–298.

Kobari, T., D. K. Steinberg, A. Ueda, A. Tsuda, M. W. Silver, and M. Kitamura. 2008. Impacts of ontogenetically migrating copepods on downward carbon flux in the western subarctic Pacific Ocean. Deep Sea Res. Part II Top. Stud. Oceanogr. **55**: 1648–1660.

Kvile, K. Ø., C. Ashjian, Z. Feng, J. Zhang, and R. Ji. 2018. Pushing the limit: Resilience of an Arctic copepod to environmental fluctuations. Glob. Chang. Biol. **24**: 5426–5439.

Laufkotter, C., and others. 2015. Drivers and uncertainties of future global marine primary production in marine ecosystem models. Biogeosciences **12**: 6955–6984.

Locarnini, R., and others. 2019. World ocean atlas, volume 1: Temperature. NOAA Atlas NESDIS.

Longhurst, A., and R. Williams. 1992. Carbon flux by seasonal vertical migrant copepods is a small number. J. Plankton Res. **14**: 1495–1509.

Maier-Reimer, E., U. Mikolajewicz, and A. Winguth. 1996. Future ocean uptake of CO_2: Interaction between ocean circulation and biology. Climate Dynam. **12**: 711–722.

Maps, F., S. Plourde, and B. Zakardjian. 2010. Control of dormancy by lipid metabolism in Calanus finmarchicus: A population model test. Mar. Ecol. Prog. Ser. **403**: 165–180.

Miller, C. B., B. W. Frost, H. P. Batchelder, M. J. Clemons, and R. E. Conway. 1984. Life histories of large, grazing copepods in a subarctic ocean gyre: *Neocalanus plumchrus*, *Neocalanus cristatus*, and *Eucalanus bungii* in the Northeast Pacific. Prog. Oceanogr. **13**: 201–243.

Miller, C. B., and M. J. Clemons. 1988. Revised life history analysis for large grazing copepods in the subarctic Pacific Ocean. Prog. Oceanogr. **20**: 293–313.

Miller, C. B., and M. Terazaki. 1989. The life histories of *Neocalanus flemingeri* and *Neocalanus plumchrus* in the sea of Japan. Bull. Plankton Soc. Jpn. **36**: 27–41.

Neelin, J. D. 2011. Climate change and climate modeling. New York Cambridge Univ. Press.

Ohman, M. D., J. M. Bradford, and J. B. Jillett. 1989. Seasonal growth and lipid storage of the circumglobal, subantarctic copepod, *Neocalanus tonsus* (Brady). Deep Sea Res. Part A Oceanogr. Res. Pap. **36**: 1309–1326.

Pinti, J., and others. 2022. The global importance of metazoans to the biological carbon pump. BioRxiv: 1–15.

Pinti, J., A. W. Visser, C. Serra-Pompei, K. H. Andersen, M. D. Ohman, and T. Kiørboe. 2022. Fear and loathing in the pelagic: How the seascape of fear impacts the biological carbon pump. Limnol. Oceanogr. **67**: 1238–1256.

Pond, D. W., G. A. Tarling, P. Ward, and D. J. Mayor. 2012. Wax ester composition influences the diapause patterns in the copepod *Calanoides acutus*. Deep Sea Res. Part II Top. Stud. Oceanogr. **59-60**: 93–104.

Record, N. R., R. Ji, F. Maps, Ø. Varpe, J. A. Runge, C. M. Petrik, and D. Johns. 2018. Copepod diapause and the biogeography of the marine lipidscape. J. Biogeogr. **45**: 2238–2251.

Richardson, A. J. 2008. In hot water: Zooplankton and climate change. ICES J. Mar. Sci. **65**: 279–295.

Richardson, A. J., and D. S. Schoeman. 2004. Climate impact on plankton ecosystems in the Northeast Atlantic. Science **305**: 1609–1612.

Saumweber, W. J., and E. G. Durbin. 2006. Estimating potential diapause duration in *Calanus finmarchicus*. Deep Sea Res. Part II Top. Stud. Oceanogr. **53**: 2597–2617.

Schlitzer, R. 2002. Carbon export fluxes in the Southern Ocean: Results from inverse modeling and comparison with satellite-based estimates. Deep Sea Res. Part II Top. Stud. Oceanogr. **49**: 1623–1644.

Serra-Pompei, C., B. A. Ward, J. Pinti, A. W. Visser, T. Kiørboe, and K. H. Andersen. 2022. Linking plankton size spectra and community composition to carbon export and its efficiency. Global Biogeochem. Cycl. **36**: e2021GB007275.

Siegel, D. A., K. O. Buesseler, S. C. Doney, S. F. Sailley, M. J. Behrenfeld, and P. W. Boyd. 2014. Global assessment of ocean carbon export by combining satellite observations and food-web models. Global Biogeochem. Cycl. **28**: 181–196.

Smith, S. L. 1982. The northwestern Indian Ocean during the monsoons of 1979: Distribution, abundance, and feeding of zooplankton. Deep Sea Res. Part A Oceanogr. Res. Pap. **29**: 1331–1353.

Swalethorp, R., S. Kjellerup, M. Dünweber, T. G. Nielsen, E. F. Møller, S. Rysgaard, and B. W. Hansen. 2011. Grazing, egg production, and biochemical evidence of differences in the life strategies of *Calanus finmarchicus*, *C. glacialis* and *C. hyperboreus* in Disko Bay, Western Greenland. Mar. Ecol. Progress Ser. **429**: 125–144.

Tarling, G. A., R. S. Shreeve, P. Ward, A. Atkinson, and A. G. Hirst. 2004. Life-cycle phenotypic composition and mortality of *Calanoides acutus* (Copepoda: Calanoida) in the Scotia Sea: A modelling approach. Mar. Ecol. Prog. Ser. **272**: 165–181.

Tsuda, A., H. Saito, and H. Kasai. 2001. Life history strategies of subarctic copepods *Neocalanus flemingeri* and *N. plumchrus*, especially concerning lipid accumulation patterns. Plankton Biol. Ecol. **48**: 52–58.

Verheye, H. M., L. Hutchings, J. A. Huggett, and S. J. Painting. 1992. Mesozooplankton dynamics in the Benguela ecosystem, with emphasis on the herbivorous copepods. S. Afr. J. Mar. Sci. **12**: 561–584.

Verheye, H. M., W. Hagen, H. Auel, W. Ekau, N. Loick, I. Rheenen, P. Wencke, and S. Jones. 2005. Life strategies, energetics and growth characteristics of *Calanoides carinatus* (Copepoda) in the Angola-Benguela frontal region. Afr. J. Mar. Sci. **27**: 641–651.

Vinogradov, M. 1962. Feeding of the deep-sea zooplankton. ICES Rep. **18**: 114–120.

Visser, A. W., and S. H. Jónasdóttir. 1999. Lipids, buoyancy and the seasonal vertical migration of *Calanus finmarchicus*. Fish. Oceanogr. **8**: 100–106.

Visser, A. W., J. Grønning, and S. H. Jónasdóttir. 2017. *Calanus hyperboreus* and the lipid pump. Limnol. Oceanogr. **62**: 1155–1165.

Voronina, N. 1975. On the ecology and biogeography of plankton of the Southern Ocean. Trudy Inst. Okeanogr. **103**: 60–87.

Ward, P., A. Atkinson, and G. Tarling. 2012. Mesozooplankton community structure and variability in the Scotia Sea: A seasonal comparison. Deep Sea Res. Part II Top. Stud. Oceanogr. **59–60**: 78–92.

Williams-Howze, J. 1997. Dormancy in the free-living copepod orders Cyclopoida, Calanoida and Harpacticoida. Oceanogr. Mar. Biol. **35**: 257–322.

Zmijewska, M. I., J. Yen, and L. Bielecka. 1999. Size variability in two common Antarctic copepods: *Calanoides acutus* (Giesbrecht) and *Metridia gerlachei* (Giesbrecht). Pol. Polar Res. **20**: 325–333.

Acknowledgments

This work was supported by the Horizon 2020 projects ECOTIP (grant agreement # 869383) and OCEAN-ICU (grant agreement #101083922) and the Centre for Ocean Life, a VKR Centre of Excellence funded by the Villum Foundation, by the Gordon and Betty Moore Foundation (grant #5479). The authors thank Michael Heath and Kristina Kvile for providing us with abundance estimates for *C. finmarchicus* and *C. hyperboreus*, respectively, and Tim DeVries for providing us with OCIM, the model that was used to compute sequestration estimates based on computed carbon export. The authors appreciate the two anonymous reviewers whose insightful suggestions helped improve the manuscript. [Corrections added on 23 March 2023, after online publication. Acknowledgments section has been revised and updated.]

Conflict of Interest

None declared

Submitted 26 August 2022
Revised 20 February 2023
Accepted 22 February 2023

Associate editor: Bingzhang Chen